Journal of Applied Biology & Biotechnology Vol. 14(3), pp. 153-164, May-June, 2026
Available online at http://www.jabonline.in
DOI: 10.7324/JABB.2026.301460

Role of Enterobacter cloacae SK1 in nickel removal and detection of nickel-resistance genes using Rapid Annotation using the Subsystem Technology server

Kasthuri Sivakumar, Shanmuga Priya Ramasamy*

Department of Microbiology, PSG College of Arts & Science, Coimbatore, Tamil Nadu, India.

ARTICLE INFO

Article history:
Received on: 04/12/2025
Accepted on: 21/02/2026
Available online: 05/04/2026

Key words:
Enterobacter cloacae SK1,
Foundry soil,
In situ bioremediation,
Nickel,
Rapid annotation using subsystem technology server.

ABSTRACT

Nickel contamination leads to serious ecological and health risks, necessitating the need for sustainable remediation strategies. This study evaluated the nickel remediation potential of *Enterobacter cloacae* SK1, which exhibited a high minimal inhibitory concentration of 1100 ppm. Optimization experiments revealed a maximum nickel removal efficiency of 92.83% under optimal conditions of 48 h of contact time, 50 ppm initial nickel concentration, pH 7, temperature of 28°C, and 1.5% biomass concentration. Fourier transform infrared spectroscopy (FTIR) analysis indicated the involvement of functional groups, such as O–H, C–H, N–O, and C–N in nickel binding. Scanning electron microscope (SEM) analysis showed cell aggregation and shrinkage in nickel-exposed cells, while Transmission electron microscope (TEM) confirmed intracellular sequestration of nickel as electron-dense granules. Further, the cells were immobilized in alginate, agarose, and chitosan, and their removal efficiencies were compared. Alginate-immobilized cells achieved the highest removal efficiency (98.33%), compared with agarose (68.17%) and chitosan (75%). FTIR spectra of alginate-immobilized *E. cloacae* SK1 revealed the involvement of various functional groups (O–H, C–H, and N–H), while SEM showed increased surface damage following nickel exposure. In an *in situ* bioremediation experiment, alginate-immobilized cells removed 93.50% of nickel from contaminated soil compared to the native cells (91.24%). Genomic analysis identified resistance genes *NiCoT*, *hupE*, and *mgtE*, confirming the strain's metal tolerance. Thus, these findings demonstrated that *E. cloacae* SK1 could be considered as a sustainable biological agent for mitigating nickel contamination in polluted environments.

1. INTRODUCTION

Human activities, such as improper industrial waste disposal, rapid urbanization, and the excessive use of fertilizers and pesticides are significant sources of heavy metal pollution in the soil ecosystem. González Henao and Ghneim-Herrera [1] reported that approximately 5 million soil sites worldwide are contaminated with heavy metals above regulatory limits. Among various anthropogenic sources of metal contamination, foundry waste plays a major role. In India, about 1.71 million tons of foundry waste are generated annually, which contaminates the soil ecosystem and causes a significant threat to the environment, as stated by Faisal *et al*. [2]. Foundry contaminated soil is of particular concern because it contains toxic metals, such as nickel. Accordingly, considerable concentrations of nickel have been detected in spent foundry soil, as reported by Cioli *et al*. [3] and Bożym [4]. The continuous release of nickel into the environment is dangerous because it accumulates in flora and fauna and ultimately threatens human health and organisms at all trophic levels [5].

In addition to environmental impacts, nickel exposure in humans can damage vital organs, such as the lungs, kidneys, heart, and skin, leading to pulmonary fibrosis, cardiovascular diseases, renal edema, and contact dermatitis. Furthermore, chronic exposure to nickel has been associated with increased risk of respiratory cancer [6]. Considering the health and environmental risks associated with nickel, its removal from the contaminated environment becomes essential. Conventional remediation methods, including soil replacement, soil spading, soil washing, electrokinetic remediation, chemical reduction, chemical stabilization, and photocatalysis, have been employed for nickel remediation. However, these techniques are often costly and damage the environment, which procures a desperate alternative. Bioremediation was chosen as the best replacement for the chemical method, as reported by El-Naggar *et al*. [7] and Gabr *et al*. [8].

The present study focused on the use of indigenous nickel-resistant bacteria for the biosorption of nickel from contaminated foundry soil. These native bacterial strains are well-adapted to the environmental conditions where they were isolated and can effectively remove nickel. To enhance the

*Corresponding Author:
Shanmuga Priya Ramasamy,
Department of Microbiology, PSG College of Arts and Science, Coimbatore, Tamil Nadu, India.
E-mail: priyajasper @ gmail.com

bacterial remediation efficiency under *in situ* conditions, the native strains were immobilized in non-toxic, supportive matrices, such as alginate, agarose, and chitosan. This approach improves the stability, reusability, and efficiency of microbes in nickel removal [9]. Besides evaluating the biosorption capacity, this study focuses on identifying critical genes responsible for nickel resistance and remediation, with emphasis on their roles in metal binding and cellular transport mechanisms. Overall, this study aimed to develop an environmentally sustainable and practically applicable bioremediation approach using immobilized bacteria for the remediation of nickel-contaminated foundry soils.

2. MATERIALS AND METHODS

2.1. Isolation and Determination of Minimal Inhibitory Concentration (MIC) of Nickel-Resistant Bacteria

The metal-resistant bacterial strain was previously isolated from metal-contaminated foundry soil and identified as *Enterobacter cloacae* SK1 through 16S rRNA gene sequencing [10]. The MIC of *E. cloacae* SK1 for nickel was determined using the plate dilution technique [11]. Sterile nickel solution ranging from 100 to 1500 ppm was aseptically mixed with nutrient agar and poured into sterile petri plates. The *E. cloacae* SK1 (0.5 McFarland standard) culture was then inoculated onto the nickel-amended plates and incubated at 37°C for 48 h. The nickel concentration that completely inhibited the bacterial growth was determined as the MIC [12].

2.2. Effect of Different Growth Parameters on Nickel Biosorption by *E. cloacae* SK1

2.2.1. Effect of contact time and initial metal ion concentration

To optimize the nickel remediation potential of the active strain, the effect of initial nickel ion concentrations ranging from 50 to 250 ppm and contact time was investigated. Each experimental flask containing nutrient broth was inoculated with 1% of *E. cloacae* SK1 (0.5 McFarland standard) and incubated at 37°C for various contact times (6, 12, 18, 24, 30, 36, 42, 48, 54, 60, 66, and 72 h) [13,14]. After incubation, samples were withdrawn at each of the above specified contact times and centrifuged at 5000 rpm for 15 min. The nickel concentration in the supernatant was analyzed by adding 1 mL of dimethylglyoxime solution, 2 mL of saturated bromine water, and 5 mL of ammonia solution (dimethylglyoxime method). Distilled water was also subjected to the above-said method served as the blank. Absorbance was then measured using a UV-Vis spectrophotometer (Visible Spectrophotometer, LABMAN, LMSP-V320, India) at a wavelength of 470 nm [15-17]. The nickel removal percentage was calculated using the following formula.

$$\text{Percentage removal} = \frac{Ci - Cf}{Ci} \times 100$$

(*Ci* is the initial nickel concentration in the medium and *Cf* is the final nickel concentration in the medium).

2.2.2. Effect of pH

The effect of pH on nickel remediation by *E. cloacae* SK1 was examined at various pH values ranging from 1 to 14. The experiments were carried out using sterile nutrient broth amended with 50 ppm of nickel. Further, the broth was inoculated with 1% of *E. cloacae* SK1 (0.5 McFarland standard) and incubated at 37°C for 48 h. After incubation, the samples were centrifuged at 5000 rpm for 15 min and analyzed by the dimethylglyoxime method [15-17].

2.2.3. Effect of temperature

To determine the optimal temperature for nickel biosorption, 1% of *E. cloacae* SK1 (0.5 McFarland standard) was inoculated into the sterile nutrient broth adjusted to pH 7, supplemented with 50 ppm of nickel, and incubated at various temperatures (18°C, 28°C, 37°C, 45°C and 55°C) for 48 h. After incubation, samples were centrifuged at 5000 rpm for 15 min, and analyzed by the dimethylglyoxime method [15-17].

2.2.4. Effect of inoculum concentration

The effect of inoculum concentration on nickel biosorption was investigated using sterile nutrient broth, adjusted to pH 7 and supplemented with 50 ppm of nickel. Inoculum concentrations ranging from 0.5% to 2.5% of *E. cloacae* SK1 (0.5 McFarland standard) were added individually and incubated at 28°C for 48 h. After incubation, samples were centrifuged at 5000 rpm for 15 min, and analyzed by the dimethylglyoxime method.

2.3. Fourier Transform Infrared Spectroscopy (FTIR) Analysis of Nickel-Untreated and Nickel-Treated Native *E. cloacae* SK1

E. cloacae SK1 was cultured in nutrient broth amended with 50 ppm nickel and incubated for 48 h at 28°C (test). Further, control was prepared without the addition of nickel. After incubation, the bacterial pellets were collected by centrifugation at 10,000 rpm for 10 min and resuspended in distilled water. The cell suspensions were then placed on a ZnSe crystal for drying and analyzed using FTIR spectroscopy (Shimadzu, Japan) in the wavelength range of 4000–400 cm^{-1} [18].

2.4. SEM Analysis of Nickel-Untreated and Nickel-Treated Native *E. cloacae* SK1

Morphological alterations in *E. cloacae* SK1 due to nickel exposure were examined using SEM. The strain was inoculated into the nutrient broth amended with 50 ppm nickel (test) and incubated for 48 h at 28°C. Further, control was prepared without the addition of nickel. After incubation, the cell cultures were centrifuged at 10,000 rpm for 10 min, washed three times with Phyto-bio system (PBS), and fixed onto a glass slide for 3 h in 3 mL of 2.5% glutaraldehyde solution. After fixation, the cells were washed 3 times with PBS and dehydrated using an ethanol gradient (30%, 50%, 70%, and 100%). The dehydrated cells were then placed on an aluminium stub for drying, mounted on a carbon-conductive sample holder, coated with platinum, and visualized under SEM (Carl Zeiss EVO 18, Germany) [19].

2.5. TEM Analysis of Nickel-Untreated and Nickel-Treated Native *E. cloacae* SK1

To investigate the intracellular accumulation of nickel in *E. cloacae* SK1, TEM was performed. *E. cloacae* SK1 cells were grown in nutrient broth containing 50 ppm nickel (test). Control was prepared without the addition of nickel. After incubation, the cells were harvested using centrifugation (10,000 rpm for 10 min), washed with PBS, and fixed for 3 h in 2.5% glutaraldehyde. After primary fixation, the samples were post-fixed with 1% osmium tetroxide at 4°C for 2 h. The fixed cells were then dehydrated through a graded ethanol series and transferred onto 200-mesh carbon-coated copper grids. After drying, the samples were examined using a TEM (JEOL JEM 2100, Japan) operated at an accelerating voltage of 200 kV [19,20].

2.6. Detection of Nickel Removal Efficiency by Alginate, Agarose, and Chitosan-Immobilized Cells of *E. cloacae* SK1

The immobilization of active bacterial strain using polymeric substances, such as alginate, agarose, and chitosan was performed, and the nickel biosorption efficiency was determined. To prepare alginate-immobilized cells of *E. cloacae* SK1, 2 g of sodium alginate

were dissolved in 60 mL of hot, sterile distilled water. Then, 2 g of *E. cloacae* SK1 biomass was added, and the total volume was adjusted to 100 mL with sterile distilled water. The resulting mixture was extruded through a 2.5 mL syringe into 100 mL of 0.2 M calcium chloride ($CaCl_2$) solution to form uniform-sized beads [21]. Agarose beads were prepared by dissolving 2 g of agarose powder in 60 mL of hot, sterile distilled water, and 2 g of *E. cloacae* SK1 biomass was added. Then the volume was made up to 100 mL with sterile distilled water. The mixture was added dropwise using a 2.5 mL syringe into paraffin oil to form agarose-immobilized beads [21]. For chitosan immobilization, 2 g of chitosan were mixed with 60 mL of acetic acid and left overnight. Thereafter, 40 mL of *E. cloacae* SK1 cell culture was added, and the mixture was extruded through a 2.5 mL syringe into 100 mL of 0.25 mol/L sodium hydroxide (NaOH) solution to form uniform-sized chitosan beads [22]. The prepared immobilized cells were then incubated individually in 50 ppm nickel-containing nutrient broth adjusted to pH 7 and incubated for 48 h at 28°C, and their biosorption efficiency was evaluated to determine the most effective polymer for nickel removal.

2.7. FTIR Analysis of Nickel-Treated and Nickel-Untreated Alginate-Immobilized Cells of *E. cloacae* SK1

Alginate-immobilized *E. cloacae* SK1 cells were cultured in nickel-amended (50 ppm) nutrient broth and incubated for 48 h at 28°C (test). Control was prepared without the addition of nickel. After incubation, the samples were centrifuged at 10,000 rpm for 10 min to obtain alginate-immobilized cell pellets and resuspended in sterile distilled water. Further, the alginate cell suspensions were placed on a ZnSe crystal for drying and analyzed using FTIR spectroscopy (Shimadzu, Japan) in the wavelength range of 4000–400 cm^{-1} [18].

2.8. SEM Analysis of Nickel-Treated and Nickel-Untreated Alginate-Immobilized Cells of *E. cloacae* SK1

Nickel-induced morphological alterations in alginate-immobilized cells of *E. cloacae* SK1, which was detected by SEM. Alginate-immobilized cells were cultivated in nickel-amended (50 ppm) nutrient broth and incubated for 48 h at 28°C (test). Control was prepared without the addition of nickel. After incubation, the resulting cultures were centrifuged at 10,000 rpm for 10 min to obtain cell pellets. Then the pellets were washed 3 times with PBS solution and fixed for 3 h using 3 mL of 2.5% glutaraldehyde solution. Following fixation, the cells were washed 3 times with PBS and dehydrated through an increased gradient of ethanol solution (30%, 50%, 70%, and 100%). Further, the cells were placed on an aluminium stub for drying and mounted on a carbon-conductive sample holder coated with platinum and visualized under SEM (Carl Zeiss EVO 18, Germany) [19].

2.9. *In situ* Bioremediation of Nickel-Contaminated Foundry Soil

The *in situ* bioremediation experiment was carried out using the method proposed by Rosariastuti *et al.* [23] with some modifications. Three experimental plots, each measuring 50 cm × 50 cm, were created in nickel-contaminated foundry soil. The initial nickel concentration in the experimental site was determined using Atomic Absorption Spectrometry (AAS, SHIMADZU, AA-6300, Japan) before the start of the experiment. Further, two plots were served as controls: One receives 10% freshly prepared native *E. cloacae* SK1 (3×10^9 CFU/g), and the other plot received 10% freshly prepared alginate beads without *E. cloacae* SK1. The 3rd treatment plot was inoculated with 10% freshly prepared alginate-immobilized *E. cloacae* SK1 (3×10^9 CFU/g). Further, the soil samples were collected on the 3rd and 5th days of treatment, and the nickel concentrations were measured using AAS (SHIMADZU, AA-6300, Japan) to examine the remediation efficiency of alginate-immobilized cells [24,25].

2.10. *In silico* Analysis: Prediction of the Nickel Resistance Genes in *E. cloacae* SK1

Genomic DNA from the nickel-resistant strain *E. cloacae* SK1 was isolated using the AlexGen bacterial DNA extraction kit (Alexius Biosciences, Germany) according to the manufacturer's protocol. The sequencing library was constructed with the Twist NGS Library Preparation Kit (South San Francisco, CA, USA). The paired-end sequencing was conducted on an Illumina NovaSeq 6000 system (San Diego, CA, USA) [26]. *In silico* genome analysis of the nickel-resistant strain *E. cloacae* SK1 was conducted using the rapid annotation using subsystem technology (RAST) server, with SEED viewer. RAST is an online tool that facilitates the identification and functional annotation of genes within the genome, allowing the prediction of key genes involved in nickel resistance and detoxification mechanisms [27].

2.11. Statistical Analysis

One-way analysis of variance (ANOVA) was conducted using the statistical package for the biological and social sciences (SPSS) (version 16.0) to analyze the significance of the data. Further, the results are expressed as mean ± standard deviation [28].

3. RESULT AND DISCUSSION

3.1. Isolation and Determination of MIC of Nickel-Resistant Bacteria

The previously isolated and identified nickel-resistant *E. cloacae* SK1 (GenBank accession number – OR835983) was used for this study. *E. cloacae* SK1 showed an MIC of 1100 ppm for nickel, demonstrating a strong ability to tolerate nickel. Pavlić *et al*. [29] reported that the nickel-resistant strains *Staphylococcus aureus* strain ATCC 29213, *Enterococcus faecalis* ATCC 29212, and *Escherichia coli* ATCC 25922 showed an MIC of 1000 ppm for nickel. In addition, Banerjee *et al*. [30] reported that the nickel-resistant *E. cloacae* B1 showed a MIC of 700 ppm for nickel. The variation in MIC was due to the differences in the genomic characteristics of the isolates, as noted by Navarro *et al*. [31] and Al-Jebouri *et al*. [32].

3.2. Effect of Different Growth Parameters on Nickel Biosorption by *E. cloacae* SK1

3.2.1. Effect of contact time and initial metal ion concentration

The influence of contact time and initial metal ion concentration on nickel removal by *E. cloacae* SK1 was illustrated in Figure 1. At 48 h of contact time, *E. cloacae* SK1 removed 90.83% of 50 ppm nickel. Beyond this optimum contact time and initial nickel ion concentration, the biosorption efficiency remained constant. Similarly, Paul and Mukherjee [33] and Bisht and Kumar [34] reported that *Enterobacter asburiae* KUNi5 and *Kluyvera cryocrescens* M7, respectively, exhibited maximum nickel removal after 48 h. De Padua and Dela Cruz [35] also found that the nickel-resistant strains removed 66–68% of nickel at a concentration of 50 ppm. At lower metal ion concentrations, increased contact time enhanced the availability of active binding sites, thereby improving nickel biosorption. However, after reaching the optimum conditions, the availability of these binding sites decreased due to saturation by metal ions, leading to repulsive forces that hindered further biosorption [36,37].

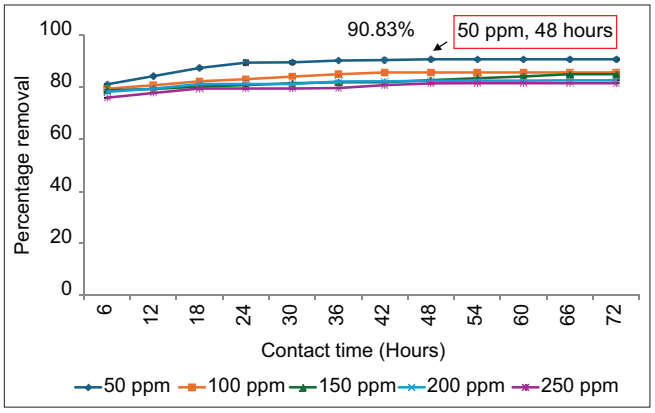

Figure 1: Effect of contact time and initial nickel ion concentration on the removal of nickel. Data are expressed as mean ± standard deviation (n = 3), (P > 0.05).

3.2.2. Effect of pH

E. cloacae SK1 was able to remove a maximal nickel removal efficiency of 90.83% at pH 7 [Figure 2], in accordance with the result reported by Paul and Mukherjee [33]. The nickel removal efficiency was increased up to pH 7, which was due to the deprotonation of functional binding sites of the bacterial cell wall, as stated by Oves *et al*. [38], Al-Fakih [39], and Gupta and Jain [40]. Similarly, Taran *et al*. [41], Oves *et al*. [38] reported that nickel-resistant bacterial strains showed optimum nickel removal at pH 7. Further, under acidic conditions, the metal binding sites were closely associated with hydronium ions (H_3O), which create repulsive forces that reduced metal binding efficiency. However, beyond pH 7, the formation of nickel hydroxide ($Ni(OH)_2$) precipitates reduced the biosorption efficiency, as reported by Yu and Jiang [42].

3.2.3. Effect of temperature

E. cloacae SK1 was able to remove 92.17% of nickel at a temperature of 28°C [Figure 3]. Similar results were observed by Haque *et al*. [43], where metal-resistant strains, such as *E. asburiae* ENSD102, *Enterobacter ludwigii* ENSH201, *Vitreoscilla* sp. ENSG301, *Acinetobacter lwoffii* ENSG302, and *Bacillus thuringiensis* ENSW401 exhibited maximum nickel removal at a temperature of 28°C. Below this optimum temperature, microbial growth and enzyme activity decreased, which consequently lowered the biosorption efficiency. Moreover, above the optimal temperature, the bacterial cell membrane structure was destroyed, leading to reduced nickel removal efficiency [44].

3.2.4. Effect of inoculum concentration on nickel removal

At an inoculum concentration of 1.5%, *E. cloacae* SK1 was able to remove 92.83% of nickel [Figure 4], due to the presence of sufficient active binding sites as reported by Ameen *et al*. [45] However, when the inoculum concentration was either increased or decreased beyond this optimum level, the nickel biosorption efficiency declined. At lower bacterial concentrations, the number of metal ions exceeded the available binding sites, which negatively affected the removal efficiency. Conversely, above the optimum inoculum concentration, aggregation of metal ions on the metal binding sites occurred, reducing the overall remediation efficacy, as stated by Chintalpudi *et al*. [36].

3.3. FTIR Analysis of Nickel-Treated and nickel-untreated native *E. cloacae* SK1

The FTIR spectra of nickel-untreated (control) and nickel-treated *E. cloacae* SK1 (test) revealed notable shifts in various functional groups, indicating their active involvement in nickel biosorption [Figure 5 and Table 1]. In the control cells, characteristic peaks corresponding to O–H, C-H, N-O, and C–N groups were observed. Upon exposure to 50 ppm nickel, shifts in these peaks were occurred, suggesting direct interaction between nickel ions and these functional groups on the bacterial cell surface. Noman *et al*. [46], Campillo-Cora *et al*. [47], and Fomina and Gadd [48] emphasized that metal ions commonly interact with the functional groups present on the microbial cell surfaces, thereby contributing to effective metal removal. Similar to our results, Paul and Mukherjee [33] reported peak shifts in O–H and C–H functional groups in nickel-treated *E. asburiae* KUNi5. Furthermore, Usmonkulova *et al*. [49] reported shifts in the C–N functional group, while Idrees *et al*. [50] observed changes in the N–O functional group upon metal interaction.

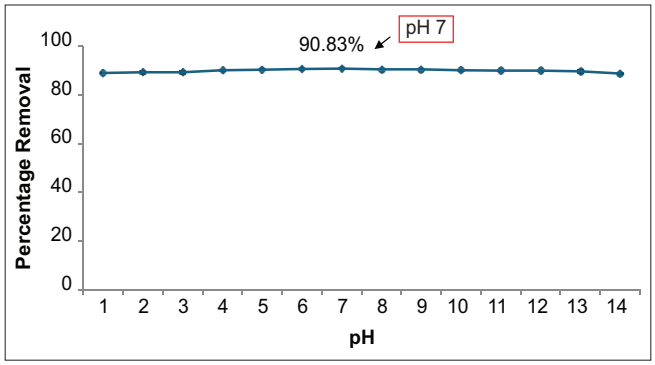

Figure 2: Effect of pH on the removal of nickel. Data are expressed as mean ± standard deviation (n = 3), (P > 0.05).

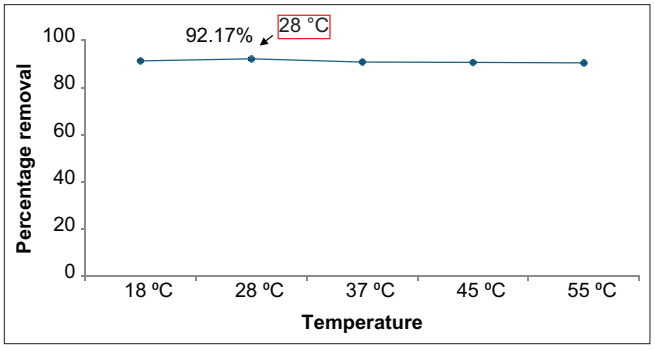

Figure 3: Effect of temperature on the removal of nickel. Data are expressed as mean ± standard deviation (n = 3), (P > 0.05).

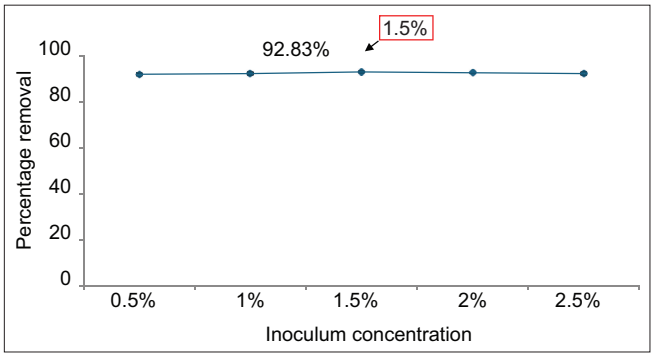

Figure 4: Effect of inoculum concentration on the removal of nickel. Data are expressed as mean ± standard deviation (n = 3), (P > 0.05).

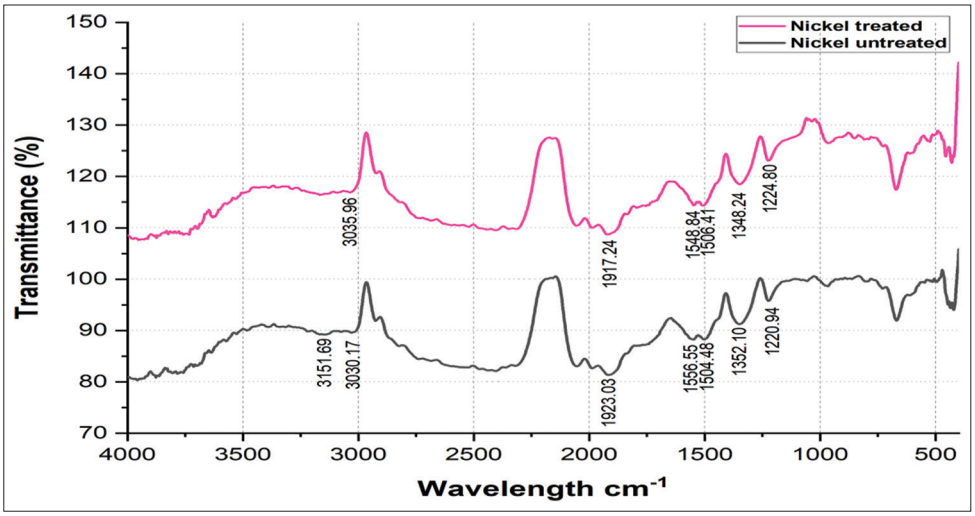

Figure 5: Fourier transform infrared spectroscopy (FTIR) analysis of nickel-treated and untreated native *Enterobacter cloacae* SK1. FTIR spectra identify functional group (O–H, C-H, N-O, and C–N) involved in nickel biosorption.

Table 1: Active functional groups involved in nickel biosorption by *Enterobacter cloacae* SK1.

Control (Nickel untreated)	Functional group	Test (Nickel treated)	Functional group	Functional group alteration due to nickel biosorption
Wavelength=(cm^{-1})		Wavelength=(cm^{-1})		
3151.69	O-H	-	-	Peak disappearance
3030.17	O-H	3035.96	O-H	O-H stretching
1923.03	C-H	1917.24	C-H	C-H bending
1556.55	N-O	1548.84	N-O	N-O stretching
1504.48	N-O	1506.41	N-O	N-O stretching
1352.10	O-H	1348.24	O-H	O-H bending
1220.94	C-N	1224.80	C-N	C-N stretching

Control: Nickel-untreated *E. cloacae* SK1; Test: Nickel-treated *E. cloacae* SK1.

Functional groups were identified using the Fourier transform infrared spectroscopy functional group table from search-InstaNANO [51].

3.4. SEM Analysis of Nickel-Treated and Nickel-Untreated Native *E. cloacae* SK1

The results showed that control cells displayed a well-defined and intact cell structure with a smooth surface [Figure 6a]. However, after exposure to nickel, significant irregularities in the cell surface were observed, due to the interactions taking place between nickel ions and the bacterial cell surface. The test cells exhibited surface shrinkage and dense cell aggregates [Figure 6b]. Similarly, Neeta *et al*. [52] reported that, under nickel exposure, *Pantoea agglomerans* JCM 1236 and *E. asburiae* JCM 6051 cells appeared as dense, aggregated structures. Further, Wang *et al*. [53] observed surface alterations in the nickel-resistant bacterial strain *Comamonas testosteroni* ZG2 after nickel exposure.

3.5. TEM Analysis of Nickel-Treated and Nickel-Untreated Native *E. cloacae* SK1

In nickel unexposed control cells, electron-lucent bacterial cells with clear internal and external surfaces were observed [Figure 7a]. However, in nickel-exposed cells, prominent electron-dense regions were detected within the cytoplasm, indicating the presence of nickel deposition [Figure 7b]. Elgamal *et al*. [54] and Nnaji *et al*. [55] reported that intracellular sequestration of heavy metals facilitated the conversion of toxic metals into less harmful forms, thereby detoxifying metal ions and reducing their availability in the surrounding environment. Similarly, Photolo *et al*. [56] and Ameen *et al*. [45] reported significant intracellular accumulation of nickel in nickel-resistant bacterial strains.

3.6. Detection of Nickel Removal Rate by Alginate, Agarose, and Chitosan-Immobilized Cells of *E. cloacae* SK1

The alginate-immobilized cells of *E. cloacae* SK1 exhibited the highest nickel removal efficiency of 98.33%, compared with agarose and chitosan-immobilized cells, which exhibited 68.17% and 75% removal of nickel, respectively [Figure 8]. Similarly, Al-Rub *et al*. [57], Ahmady-Asbchin and Bahrami [58], and Barquilha *et al*. [59] reported that alginate-immobilized cells removed higher concentration of nickel than native cells. The enhanced nickel removal efficiency of alginate-immobilized cells is due to the effective surface sorption properties of alginate, which play a key role in nickel remediation. Moreover, alginate offers several advantages, including ease of preparation process, biocompatibility, and the ability to maintain cell viability within its matrix [57]. In contrast, chitosan exhibited lower removal efficiency and had certain limitations, such as poor mechanical and thermal strength; it also required physical or chemical modification before application in remediation and was pH-sensitive, as stated by Zhang *et al.* [60] and Hsu *et al.* [61]. Agarose beads were hydrophilic and chemically and physically inert in nature,

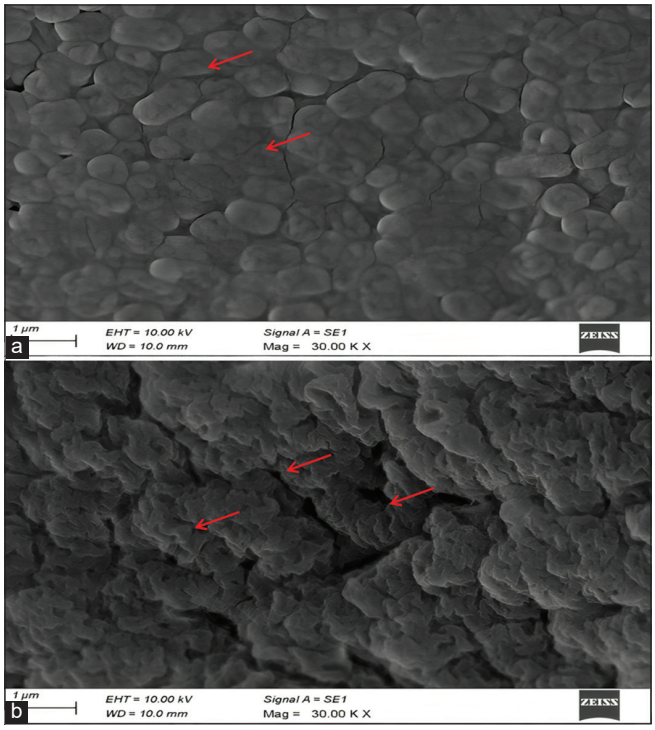

Figure 6: SEM images of *Enterobacter cloacae* SK1 (a) nickel-untreated cells (control), (b) nickel-treated cells (test). Scale bar represents 1 µm. (a) smooth, intact surfaces, whereas (b) significant surface irregularities and structural damage indicated by red arrows.

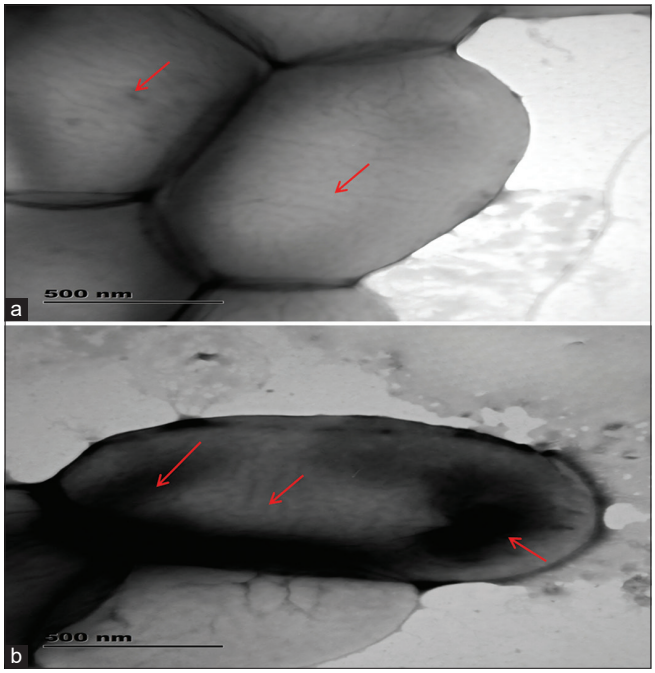

Figure 7: TEM images of *Enterobacter cloacae* SK1 (a) nickel untreated cells (control), (b) nickel treated cells (test). Scale bar represents 500 nm. (b) Intracellular accumulation of nickel, seen as electron dense region indicated by red arrow, whereas (a) absence of nickel accumulation.

as stated by Zucca *et al.* [62]. Due to the superior nickel removal performance of alginate-immobilized cells when compared to other immobilized polymers (chitosan and agarose), alginate-immobilized

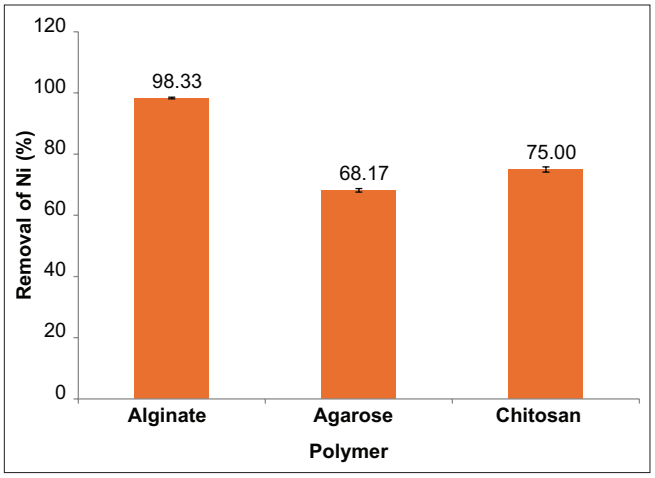

Figure 8: Nickel removal by alginate, agarose and chitosan immobilized cells of *Enterobacter cloacae* SK1. Alginate immobilized cells showed the highest nickel removal (98.33%), followed by chitosan (75%) and agarose (68.17%). Data are expressed as mean ± standard deviation ($n = 3$), ($P > 0.05$).

E. cloacae SK1 cells were selected for the *in situ* remediation study of nickel-contaminated foundry soil.

3.7. FTIR Analysis of Nickel-Treated and Nickel-Untreated Alginate-Immobilized Cells of *E. cloacae* SK1

The FTIR spectra of nickel-untreated alginate-immobilized cells showed a shift in various peaks corresponding to the functional groups, including O-H, C-H, and N-H, compared with control cells, which suggested that these functional groups play a crucial role in nickel bioremediation [Figure 9 and Table 2]. These negatively charged functional groups are likely to interact with the positively charged nickel ions, as stated by Chirizzi *et al.* [63], which paved the way for effective nickel remediation. Further, Petrovič and Simonič [64] reported that nickel exposed in alginate-immobilized cells induced the stretching in several functional groups, including O-H, C-O, C-N, and N-H, which contributed to nickel biosorption.

3.8. SEM Analysis of Nickel-Treated and Nickel-Untreated Alginate-Immobilized Cells of *E. cloacae* SK1

The SEM analysis of control cells revealed a uniform, heterogeneous, and fibrillar surface due to the incorporation of active cells into the alginate matrix, which increases the surface area and active binding sites for nickel adsorption, as stated by Khandelwal *et al.* [65]. Upon exposure to nickel, some morphological changes were observed in the alginate-immobilized *E. cloacae* SK1 (test), which include increased surface roughness, visible cracks, and greater irregularities compared with the control [Figure 10]. Similar alterations in surface morphology were noted by Naskar and Bera [66] and Petrovič and Simonič [64], who found that nickel-exposed alginate-immobilized cells exhibited a rougher texture than non-exposed cells.

3.9. *In situ* Bioremediation of Nickel-Contaminated Foundry Soil

Initially, the nickel concentration in the contaminated foundry soil was 4.0915 ppm, as determined by AAS. The *in situ* bioremediation study demonstrated that nickel removal was higher on the 5th day of treatment [Figure 11] compared to the 3rd day. Alginate-immobilized *E. cloacae* SK1 cells removed 93.50% (0.2661 ppm) of nickel, whereas native *E. cloacae* SK1 cells (control) removed only 91.24% (0.3586 ppm), and

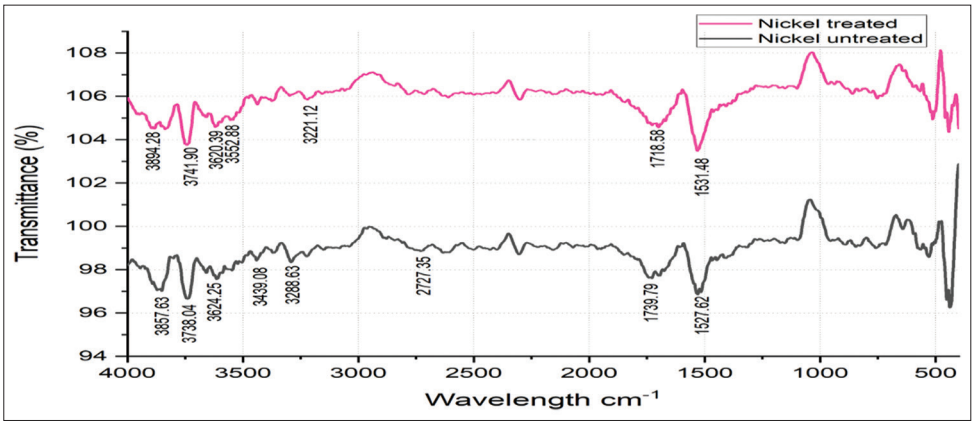

Figure 9: Fourier transform infrared spectroscopy analysis of alginate immobilized cells of *E. cloacae* SK1. FTIR spectra identify functional group (O-H, C-H, and N-H) involved in nickel biosorption by alginate immobilized cells of *E. cloacae* SK1.

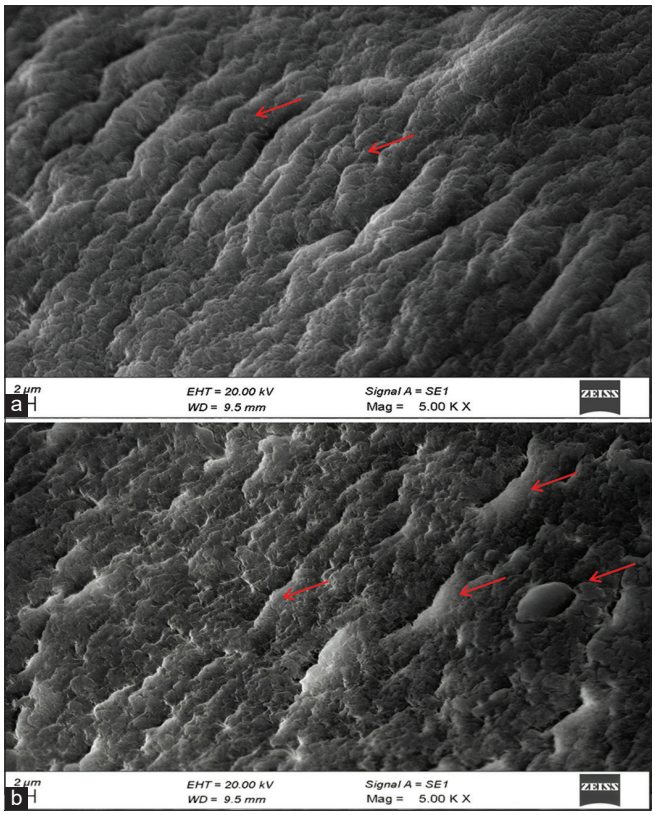

Figure 10: SEM images of alginate immobilized cells of *Enterobacter cloacae* SK1 (a) nickel-untreated cells (b) nickel-treated cells. Scale bar represents 2 µm. (b) morphological alterations and increased surface roughness compared with Figure 10a indicated by red arrow.

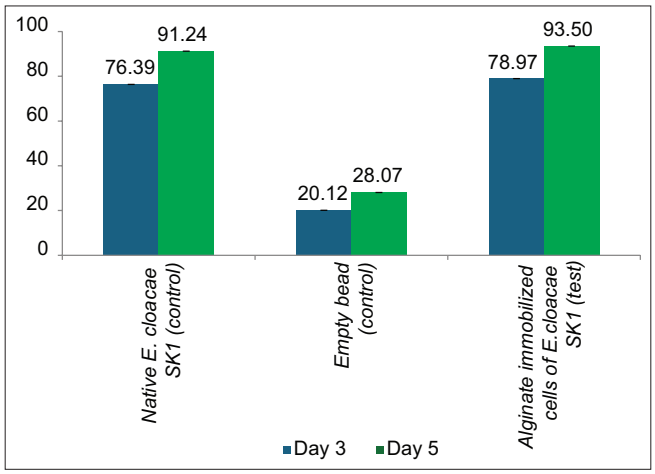

Figure 11: *In situ* nickel remediation of foundry soil at day 3 and 5. Data are expressed as mean ± standard deviation ($n = 3$), ($P > 0.05$).

empty alginate beads removed only 20.12% (2.9432 ppm) on the 5th day of treatment. Ravanbakhsh *et al*. [67] reported that bacterial strains immobilized in alginate were more effective in nickel remediation than free-living native bacterial cells. This enhanced performance can be attributed to the fact that alginate is a biodegradable and non-toxic polymer that effectively supports bacterial growth within the beads. In addition, alginate protects bacterial cells from adverse environmental conditions, thereby increasing their resistance to metal toxicity, as highlighted by El Bestawy [68]. Furthermore, alginate is composed of β-1,4-linked D-mannuronic and L-guluronic acid monomer units, which provide additional binding sites for metal adsorption facilitating nickel biosorption, as noted by Ahmady-Asbchin and Bahrami [58].

3.10. *In silico* Analysis: Prediction of the Nickel Resistance Genes in *E.cloacae* SK1

The complete genome of the strain, with a size of 4,841,549 bp, was sequenced, and gene annotation using the RAST server identified several genes associated with nickel resistance and remediation, including *NiCoT*, *hupE*, and *mgtE* [Figure 12 and Table 3]. The *NiCoT* gene acts as a nickel transporter and belongs to the HoxN/HupN/NixA family of transporters. Pathak *et al*. [69] reported that the *NiCoT* gene has a high affinity for nickel/cobalt transporter-permease enzyme in bacterial strains. Zhang *et al*. [70] described that NiCoT (HoxN/HupN/NixA) is a secondary transporter which actively involved in the transportation of nickel ions. Nickel was effectively transported across the cytoplasmic membrane of bacterial cells through secondary nickel and cobalt transporters. The NiCoT transporters possess an eight-helix structure with conserved motifs located within the transmembrane domains of various microorganisms, which play a significant role in intracellular nickel accumulation, as noted by Hebbeln and Eitinger [71], Pishchik *et al*. [72], and Xavier *et al*. [73]. Similarly, Janssen *et al*. [74] identified the presence of the *NiCoT* gene in the genome of the nickel-resistant strain *Cupriavidus metallidurans* CH34.

Table 2: Active functional groups involved in nickel biosorption by alginate-immobilized cells of *Enterobacter cloacae* SK1.

Control (Nickel-untreated)	Functional group	Test (Nickel-treated)	Functional group	Functional group alteration due to nickel biosorption
Wavelength=(cm^{1})		Wavelength=(cm^{-1})		
3857.63	O-H	3894.28	O-H	O-H stretching
3738.04	O-H	3741.90	O-H	
3624.25	O-H	3620.39	O-H	
-	O-H	3552.88	O-H	New peak formation
3439.08	O-H	-	-	Peak disappearance
3288.63	O-H	3221.12	O-H	O-H stretching
2727.35	O-H	-	-	Peak disappearance
1739.79	C-H	1718.58	C-H	C-H bending
1572.62	N-H	1531.48	N-H	N-H bending

Control: Nickel-untreated alginate-immobilized cells of *E. cloacae* SK1; Test: Nickel-treated alginate-immobilized cells of *E. cloacae* SK1.
Functional groups were identified using the Fourier transform infrared spectroscopy functional group table from Search-InstaNANO [51].

Table 3: Detection of nickel-resistant genes and its function in the genome of *Enterobacter cloacae* SK1.

Genes	Description/function	Scaffold no	Start (bp)	Stop (bp)	Location (gene number)
NiCoT (hoxN/ hupN/nixA)	Transport of Nickel and Cobalt; HoxN/HupN/NixA family, nickel/ cobalt transporter.	23	24437	23415	fig|6666666.1274357.peg. 2004
hupE	Transport of Nickel and Cobalt; HupE/UreJ family metal transporter.	5	113720	114259	fig|6666666.1274357.peg. 3616
mgtE	Mg/Co/Ni transporter/cystathionine β-synthase domain	2	68900	67899	fig|6666666.1274357.peg. 1498

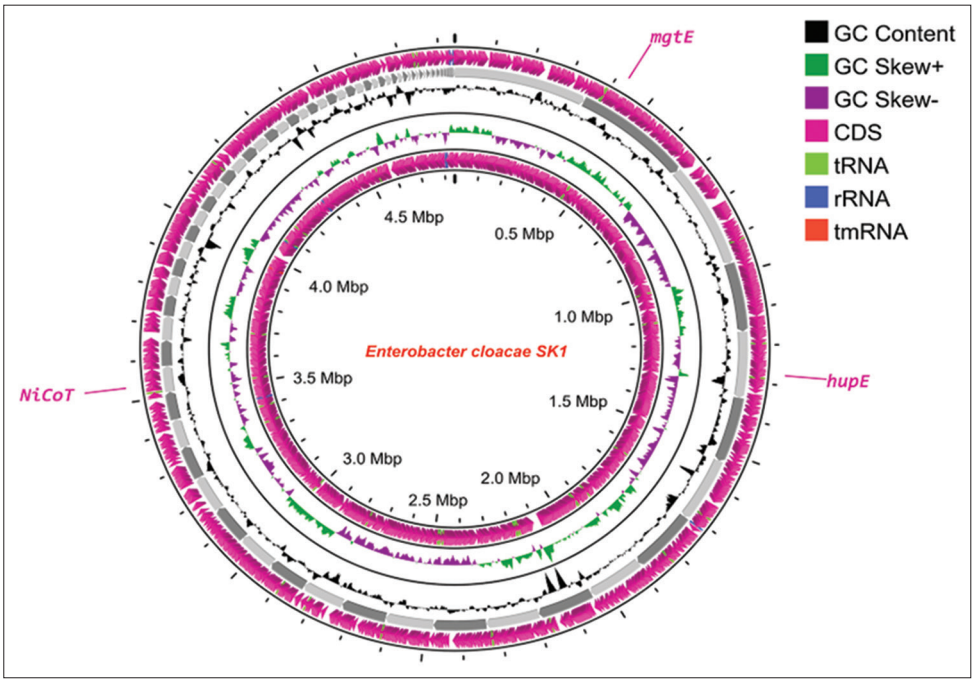

Figure 12: Circular genome map of *Enterobacter cloacae* SK1 showing the distribution of nickel resistance-related genes identified using the rapid annotation using subsystem technology server. The genome contains nickel resistance and transport genes, including *NiCoT*, *hupE*, and *mgtE*.

Another important secondary nickel and cobalt transporter gene is *hupE*, which belongs to the HupE/UreJ family transporters. This gene contributes to nickel resistance through intracellular nickel accumulation, as highlighted by Pathak *et al*. [69]. Brito *et al*. [75] suggested that the HupE/UreJ family transporters present in a wide range of bacteria and contain conserved amino acid sequence motifs that are necessary for nickel transport. Further, these transporters play an important role in enzymes, such as *NiFe* hydrogenase and urease, both of which require nickel ions for their function. Initially, the HupE transporter is synthesized as a precursor protein and later matured into a fully functional protein form with six transmembrane domains responsible for nickel uptake and accumulation, according to Huertas *et al*. [76]. Furthermore, Brito *et al*. [75] found that the *hupE* gene significantly enhanced nickel uptake in the *E. coli* mutant strain HYD723.

The *mgtE* gene acts as a magnesium, cobalt, and nickel transporter and functions as a non-selective cation channel facilitating nickel influx, as reported by Schürmann *et al*. [77]. *MgtE* is a homodimer protein present

in the cell membrane with a C-terminal tail containing cystathionine β-synthase domains, and mediates nickel transport, as described by Chen *et al*. [78] and Franken *et al*. [79]. Further, Hovorukha *et al*. [80] and Jin *et al*. [81] stated that the MgtE transporter typically facilitates nickel transport across the bacterial cell membrane.

4. CONCLUSION

This study confirmed that heavy metal bioremediation using indigenous bacteria could be a promising, environmentally sustainable approach for mitigating nickel contamination in foundry soil. The findings emphasized the importance of selecting native, metal-tolerant microorganisms to improve remediation efficiency under real field conditions. The use of polymer-based immobilization further strengthened this approach by enhancing microbial stability, protection, and efficiency. In particular, alginate emerged as a suitable immobilization matrix due to its biocompatibility, non-toxicity, and ability to support bacterial activity in contaminated environments. The identification of essential nickel resistance genes also provided valuable insights into the genetic basis of metal tolerance and transport, reinforcing the reliability of this strain for long-term remediation practices. Overall, the integration of microbial immobilization with genetic characterization offered a strong framework for developing effective and eco-friendly strategies to rehabilitate nickel-contaminated soils. This approach contributed to sustainable environmental management and represented a viable alternative to conventional methods that are costly and environmentally damaging.

5. AUTHORS' CONTRIBUTIONS

All authors made substantial contributions to conception and design, acquisition of data, or analysis and interpretation of data; took part in drafting the article or revising it critically for important intellectual content; agreed to submit to the current journal; gave final approval of the version to be published; and agree to be accountable for all aspects of the work. All the authors are eligible to be authors as per the International Committee of Medical Journal Editors (ICMJE) requirements/guidelines.

6. FUNDING

There is no funding to report.

7. CONFLICTS OF INTEREST

The authors report no financial or any other conflicts of interest in this work.

8. ETHICAL APPROVALS

This study does not involve experiments on animals or human subjects.

9. DATA AVAILABILITY

All the data are available with the authors and shall be provided upon request.

10. PUBLISHER'S NOTE

All claims expressed in this article are solely those of the authors and do not necessarily represent those of the publisher, the editors, and the reviewers. This journal remains neutral with regard to jurisdictional claims in published institutional affiliation.

11. USE OF ARTIFICIAL INTELLIGENCE (AI)-ASSISTED TECHNOLOGY

The authors declare that they have not used artificial intelligence (AI)-tools for writing and editing of the manuscript, and no images were manipulated using AI.

REFERENCES

1. Gonzalez Henao S, Ghneim-Herrera T. Heavy metals in soils and the remediation potential of bacteria associated with the plant microbiome. Front Environ Sci. 2021;9:604216. https://doi.org/10.3389/fenvs.2021.604216
2. Faisal AA, Al-Ridah ZA, Naji LA, Naushad M, El-Serehy HA. Waste foundry sand as permeable and low permeable barrier for restriction of the propagation of lead and nickel ions in groundwater. J Chem. 2020;2020(1):4569176. https://doi.org/10.1155/2020/4569176
3. Cioli F, Abbà A, Alias C, Sorlini S. Reuse or disposal of waste foundry sand: An insight into environmental aspects. Appl Sci. 2022;12(13):6420. https://doi.org/10.3390/app12136420
4. Bożym M. The study of heavy metals leaching from waste foundry sands using a one-step extraction. E3S Web Conf. 2017;19:02018. https://doi.org/10.1051/e3sconf/20171902018
5. Anusha P, Natarajan D. Bioremediation potency of multi metal tolerant native bacteria *Bacillus cereus* isolated from bauxite mines, Kolli Hills, Tamilnadu-A lab to land approach. Biocatal Agric Biotechnol. 2020;25:101581. https://doi.org/10.1016/j.bcab.2020.101581
6. Genchi G, Carocci A, Lauria G, Sinicropi MS, Catalano A. Nickel: Human health and environmental toxicology. Int J Environ Res Public Health. 2020;17(3):679. https://doi.org/10.3390/ijerph17030679
7. El-Naggar A, Ahmed N, Mosa A, Niazi NK, Yousaf B, Sharma A, *et al*. Nickel in soil and water: Sources, biogeochemistry, and remediation using biochar. J Hazard Mater. 2021;419:126421. https://doi.org/10.1016/j.jhazmat.2021.126421
8. Gabr RM, Hassan SH, Shoreit AA. Biosorption of lead and nickel by living and non-living cells of *Pseudomonas aeruginosa* ASU 6a. Int Biodeter Biodegrad. 2008;62(2):195-203. https://doi.org/10.1016/j.ibiod.2008.01.008
9. Blaga AC, Zaharia C, Suteu D. Polysaccharides as support for microbial biomass-based adsorbents with applications in removal of heavy metals and dyes. Polymers (Basel). 2021;13(17):2893. https://doi.org/10.3390/polym13172893
10. Khashei S, Etemadifar Z, Rahmani HR. Immobilization of *Pseudomonas putida* PT in resistant matrices to environmental stresses: A strategy for continuous removal of heavy metals under extreme conditions. Ann Microbiol. 2018;68(12):931-42. https://doi.org/10.1007/s13213-018-1402-7
11. Bhardwaj R, Gupta A, Garg JK. Impact of heavy metals on inhibitory concentration of *Escherichia coli*-a case study of river Yamuna system, Delhi, India. Environ Monit Assess 2018;190(11):674. https://doi.org/10.1007/s10661-018-7061-0
12. Sharma R, Talukdar D, Bhardwaj S, Jaglan S, Kumar R, Kumar R, *et al*. Bioremediation potential of novel fungal species isolated from wastewater for the removal of lead from liquid medium. Environ Technol Innov. 2020;18:100757. https://doi.org/10.1016/j.eti.2020.100757
13. Singh RR, Tipre DR, Dave SR. Optimization of Cu, Hg and Cd removal by *Enterobacter cloacae* by ferric ammonium citrate precipitation. Adv Environ Res. 2014;3(4):283-92. https://doi.org/10.12989/aer.2014.3.4.283
14. Sonawdekar S, Gupte A. Biosorption of copper (II) and cadmium (II) by *Bacillus cereus* sys1 isolated from oil-contaminated site. SN Appl Sci. 2020;2(7):1254. https://doi.org/10.1007/s42452-020-3062-z
15. García R, Campos J, Cruz JA, Calderón ME, Raynal ME, Buitrón G.

Biosorption of Cd, Cr, Mn, and Pb from aqueous solutions by *Bacillus* sp strains isolated from industrial waste activate sludge. Tip Rev Esp Cien Quím Biol. 2016;19(1):5-14. https://doi.org/10.1016/j.recqb.2016.02.001

16. Aslam F, Yasmin A, Sohail S. Bioaccumulation of lead, chromium, and nickel by bacteria from three different genera isolated from industrial effluent. Int Microbiol. 2020;23(2):253-61. https://doi.org/10.1007/s10123-019-00098-w
17. Sarkar D, Paul G. Bioremediation of nickel ions from aqueous system by dry cells of *Pseudomonas aeruginosa* DSGPM4 species. Int J Pharm Life Sci. 2015;6(1):4110-4.
18. Kepenek ES, Severcan M, Gozen AG, Severcan F. Discrimination of heavy metal acclimated environmental strains by chemometric analysis of FTIR spectra. Ecotoxicol Environ Saf. 2020;202:110953. https://doi.org/10.1016/j.ecoenv.2020.110953
19. Mohapatra RK, Parhi PK, Pandey S, Bindhani BK, Thatoi H, Panda CR. Active and passive biosorption of Pb (II) using live and dead biomass of marine bacterium *Bacillus xiamenensis* PbRPSD202: Kinetics and isotherm studies. J Environ Manage. 2019;247:121-34. https://doi.org/10.1016/j.jenvman.2019.06.073
20. Salih LI, Rasheed RO, Muhammed SM. *Raoultella ornithinolytica* as a potential candidate for bioremediation of heavy metal from contaminated environments. J Microbiol Biotechnol. 2023;33(7):895. https://doi.org/10.4014/jmb.2212.12045
21. Akhtar K, Khalid AM, Akhtar MW, Ghauri MA. Removal and recovery of uranium from aqueous solutions by Ca-alginate immobilized *Trichoderma harzianum*. Bioresour Technol. 2009;100(20):4551-8. https://doi.org/10.1016/j.biortech.2009.03.073
22. Ting LI, Hui WA, Xin-Jiang HU, Yi-Ming GU, Yuan HE. Biosorption of copper (II) from aqueous solution by *Bacillus subtilis* cells immobilized into chitosan beads. Trans Nonferrous Met Soc China. 2013;23(6):1804-14. https://doi.org/10.1016/s1003-6326(13)62664-3
23. Rosariastuti R, Maisyarah S, Sudadi S, Hartati S, Purwanto P. Remediation of chromium contaminated soil by Phyto-bio system (PBS) application. SAINS TANAH J Soil Sci Agroclimatol. 2019;16(1):90-102. https://doi.org/10.20961/stjssa.v16i1.24932
24. Sudarsan JS, Prasanna K, Kishorekumar P, Mohan SS, Nithiyanantham S. Removal of heavy metal from casting sand in valve manufacturing industry through bioremediation technique. Sustain. Water Resour Manag. 2015;1(3):263-6. https://doi.org/10.1007/s40899-015-0023-6
25. Fauziah SH, Jayanthi B, Emenike CU, Agamuthu C. Remediation of heavy metal contaminated soil using potential microbes isolated from a closed disposal site. Int J Biosci Biochem Bioinform. 2017;7(4):230-7. https://doi.org/10.17706/ijbbb.2017.7.4.230-237
26. Iram D, Sansi MS, Puniya AK, Meena S, Vij S. Draft genome sequence of methicillin-resistant *Staphylococcus aureus* strain D1418m22 isolated from human wound pus. Microbiol Resour Announc. 2023;12(11):e0040923. https://doi.org/10.1128/mra.00409-23
27. Abdullahi S, Haris H, Zarkasi KZ, Amir HG. Complete genome sequence of plant growth-promoting and heavy metal-tolerant *Enterobacter tabaci* 4M9 (CCB-MBL 5004). J Basic Microbiol. 2021;61(4):293-304. https://doi.org/10.1002/jobm.202000695
28. Nwaehiri UL, Akwukwaegbu PI, Nwoke BE. Bacterial remediation of heavy metal polluted soil and effluent from paper mill industry. Environ Anal Health Toxicol. 2020;35(2):e2020009. https://doi.org/10.5620/eaht.e2020009
29. Pavlić A, Gobin I, Begić G, Tota M, Abram M, Špalj S. The effect of nickel ions on the susceptibility of bacteria to ciprofloxacin and ampicillin. Folia Microbiol (Praha). 2022;67(4):649-57. https://doi.org/10.1007/s12223-022-00960-x
30. Banerjee G, Pandey S, Ray AK, Kumar R. Bioremediation of heavy metals by a novel bacterial strain *Enterobacter cloacae* and its antioxidant enzyme activity, flocculant production, and protein expression in presence of lead, cadmium, and nickel. Water Air Soil Pollut. 2015;226(4):91-9. https://doi.org/10.1007/s11270-015-2359-9
31. Navarro CA, von Bernath D, Jerez CA. Heavy metal resistance strategies of acidophilic bacteria and their acquisition: Importance for biomining and bioremediation. Biol Res. 2013;46(4):363-71. https://doi.org/10.4067/s0716-97602013000400008
32. Al-Jebouri MM, Al-Samarrai AH, Abdeljabar RA. Estimation of resistance to heavy metals of bacterial pathogens causing respiratory infections among workers of Al-Baiji Oil Refinery in Iraq. World J Pharm Res. 2014;3(3):3537-51.
33. Paul A, Mukherjee SK. *Enterobacter asburiae* KUNi5, a nickel resistant bacterium for possible bioremediation of nickel contaminated sites. Pol J Microbiol. 2016;65(1):115-8. https://doi.org/10.5604/17331331.1197284
34. Bisht H, Kumar N. Characterization and evaluation of the nickel-removal capacity of *Kluyvera cryocrescens* m7 isolated from industrial wastes. Pollution. 2023;9(3):1059-73. https://doi.org/10.22059/poll.2023.347580.1586
35. De Padua JC, dela Cruz TE. Isolation and characterization of nickel-tolerant *Trichoderma* strains from marine and terrestrial environments. J Fungi (Basel). 2021;7(8):591. https://doi.org/10.3390/jof7080591
36. Chintalpudi VK, Kanamarlapudi RK, Mallu UR, Muddada S. Isolation, identification, biosorption optimization, characterization, isotherm, kinetic and application of novel bacterium *Chelatococcus* sp. biomass for removal of Pb (II) ions from aqueous solutions. Int J Environ Sci Technol. 2022;19(3):1531-44. https://doi.org/10.1007/s13762-021-03169-6
37. Heidari P, Mazloomi F, Sanaeizade S. Optimization study of nickel and copper bioremediation by *Microbacterium oxydans* strain CM3 and CM7. Soil Sediment Contam. 2020;29(4):438-51. https://doi.org/10.1080/15320383.2020.1738335
38. Oves M, Khan MS, Zaidi A. Biosorption of heavy metals by *Bacillus thuringiensis* strain OSM29 originating from industrial effluent contaminated north Indian soil. Saudi J Biol Sci. 2013;20(2):121-9. https://doi.org/10.1016/j.sjbs.2012.11.006
39. Al-Fakih AA. Biosorption of Ni^{2+} and Cd^{2+} from aqueous solutions using NaOH-treated biomass of *Eupenicillium ludwigii*: Equilibrium and mechanistic studies. Open J Appl Sci. 2015;5(7):376-92. https://doi.org/10.4236/ojapps.2015.57038
40. Gupta S, Jain AK. Biosorption of Ni (II) from aqueous solutions and real industrial wastewater using modified *A. barbadensis* Miller leaves residue powder in a lab scale continuous fixed bed column. Clean Eng Technol. 2021;5:100349. https://doi.org/10.1016/j.clet.2021.100349
41. Taran M, Sisakhtnezhad S, Azin T. Biological removal of nickel (II) by *Bacillus* sp. KL1 in different conditions: Optimization by Taguchi statistical approach. Pol J Chem Technol. 2015;17(3):29-32. https://doi.org/10.1515/pjct-2015-0046
42. Yu X, Jiang J. Phosphate microbial mineralization removes nickel ions from electroplating wastewater. J Environ Manage. 2019;245:447-53. https://doi.org/10.1016/j.jenvman.2019.05.091
43. Haque MM, Mosharaf MK, Haque MA, Tanvir MZ, Alam MK. Biofilm formation, production of matrix compounds and biosorption of copper, nickel and lead by different bacterial strains. Front Microbiol. 2021;12:615113. https://doi.org/10.3389/fmicb.2021.615113
44. Wu M, Li Y, Li J, Wang Y, Xu H, Zhao Y. Bioreduction of hexavalent chromium using a novel strain CRB-7 immobilized on multiple materials. J Hazard Mater. 2019;368:412-20. https://doi.org/10.1016/j.jhazmat.2019.01.059
45. Ameen FA, Hamdan AM, El-Naggar MY. Assessment of the heavy metal bioremediation efficiency of the novel marine lactic acid bacterium, *Lactobacillus plantarum* MF042018. Sci Rep. 2020;10(1):314. https://doi.org/10.1038/s41598-019-57210-3

46. Noman E, Al-Gheethi A, Mohamed RM, Al-Sahari M, Hossain MS, Vo DV, *et al*. Sustainable approaches for nickel removal from wastewater using bacterial biomass and nanocomposite adsorbents: A review. Chemosphere. 2022;291:132862. https://doi.org/10.1016/j.chemosphere.2021.132862
47. Campillo-Cora C, Rodríguez-Seijo A, Pérez-Rodríguez P, Fernández-Calviño D, Santás-Miguel V. Effect of heavy metal pollution on soil microorganisms: Influence of soil physicochemical properties. A systematic review. Eur J Soil Biol. 2025;124:103706. https://doi.org/10.1016/j.ejsobi.2024.103706
48. Fomina M, Gadd GM. Biosorption: Current perspectives on concept, definition and application. Bioresour Technol. 2014;160:3-14. https://doi.org/10.1016/j.biortech.2013.12.102
49. Usmonkulova A, Malusa E, Kadirova G, Khalilov I, Canfora L, Abdulmyanova L. Ni^{2+} and Cd^{2+} biosorption capacity and redox-mediated toxicity reduction in bacterial strains from highly contaminated soils of Uzbekistan. Microorganisms. 2025;13(7):1485. https://doi.org/10.3390/microorganisms13071485
50. Idrees M, Ali S, Rehman A, Hussain SZ, Bukhari DA. Uptake of lead by bacteria isolated from industrial effluents and their potential use in bioremediation of wastewater. Saudi J Biol Sci. 2023;30(8):103740. https://doi.org/10.1016/j.sjbs.2023.103740
51. FTIR Functional Group Database Table with Search - InstaNANO. Available from: https://instanano.com/all/characterization/ftir/ftir-functional-group-search [Last accessed on 2025 Nov 25].
52. Neeta B, Maansi V, Harpreet SB. Characterization of heavy metal (cadmium and nickel) tolerant Gram negative enteric bacteria from polluted Yamuna River, Delhi. Afr J Microbiol Res. 2016;10(5):127-37. https://doi.org/10.5897/ajmr2015.7769
53. Wang C, Sun X, Chen Y, Zhang Y, Li M. Comparative metabolomic analysis reveals Ni (II) stress response mechanism of *Comamonas testosteroni* ZG2. Ecotoxicol Environ Saf. 2023;263:115244. https://doi.org/10.1016/j.ecoenv.2023.115244
54. Elgamal MS, Ahmed AF, Abdelbary S. Evaluation of nickel tolerance by identified *Pseudomonas aeruginosa* isolated from Egyptian polluted soils. Biosci Res. 2018;15(1):518-29.
55. Nnaji ND, Anyanwu CU, Miri T, Onyeaka H. Mechanisms of heavy metal tolerance in bacteria: A review. Sustainability. 2024;16(24):11124. https://doi.org/10.3390/su162411124
56. Photolo MM, Sitole L, Mavumengwana V, Tlou MG. Genomic and physiological investigation of heavy metal resistance from plant endophytic *Methylobacterium radiotolerans* MAMP 4754, isolated from *Combretum erythrophyllum*. Int J Environ Res Public Health. 2021;18(3):997. https://doi.org/10.3390/ijerph18030997
57. Al-Rub FA, El-Naas MH, Benyahia F, Ashour I. Biosorption of nickel on blank alginate beads, free and immobilized algal cells. Proc Biochem. 2004;39(11):1767-73. https://doi.org/10.1016/j.procbio.2003.08.002
58. Ahmady-Asbchin S, Bahrami AM. Nickel biosorption by immobilized biomass of *Bacillu*s sp. from aqueous solution. Adv Environ Biol. 2011;5:1656-62.
59. Barquilha CE, Cossich ES, Tavares CR, Silva ED. Biosorption of nickel (II) and copper (II) ions in batch and fixed-bed columns by free and immobilized marine algae *Sargassum* sp. J Clean Prod. 2017;150:58-64. https://doi.org/10.1016/j.jclepro.2017.02.199
60. Zhang Y, Zhao M, Cheng Q, Wang C, Li H, Han X, *et al*. Research progress of adsorption and removal of heavy metals by chitosan and its derivatives: A review. Chemosphere. 2021;279:130927. https://doi.org/10.1016/j.chemosphere.2021.130927
61. Hsu CY, Ajaj Y, Mahmoud ZH, Ghadir GK, Alani ZK, Hussein MM, *et al*. Adsorption of heavy metal ions use chitosan/graphene nanocomposites: A review study. Results Chem. 2024;7:101332. https://doi.org/10.1016/j.rechem.2024.101332
62. Zucca P, Fernandez-Lafuente R, Sanjust E. Agarose and its derivatives as supports for enzyme immobilization. Molecules. 2016;21(11):1577. https://doi.org/10.3390/molecules21111577
63. Chirizzi D, Mastrogiacomo D, Semeraro P, Milano F, De Bartolomeo AR, Trotta M, *et al*. Nickel ion extracellular uptake by the phototrophic bacterium *Rhodobacter sphaeroides*: New insights from Langmuir modelling and X-ray photoelectron spectroscopic analysis. Appl Surf Sci. 2022;593:153385. https://doi.org/10.1016/j.apsusc.2022.153385
64. Petrovič A, Simonič M. Removal of heavy metal ions from drinking water by alginate-immobilised *Chlorella sorokiniana*. Int J Environ Sci Technol. 2016;13(7):1761-80. https://doi.org/10.1007/s13762-016-1015-2
65. Khandelwal R, Keelka S, Jain N, Jain P, Kumar Sharma M, Kaushik P. Biosorption of arsenic (III) from aqueous solution using calcium alginate immobilized dead biomass of *Acinetobacter* sp. strain Sp2b. Sci Rep. 2024;14(1):9972. https://doi.org/10.1038/s41598-024-60329-7
66. Naskar A, Bera D. Mechanistic exploration of Ni (II) removal by immobilized bacterial biomass and interactive influence of coexisting surfactants. Environ Prog Sustain Energy. 2018;37(1):342-54. https://doi.org/10.1002/ep.12685
67. Ravanbakhsh S, Anita K, Azam T. Cadmium, nickel and vanadium accumulation by three strains of marine bacteria. Iran J Biotechnol. 2024;4(3):180-7.
68. El Bestawy E. Efficiency of immobilized cyanobacteria in heavy metals removal from industrial effluents. Desalination Water Treat. 2019;159:66-78. https://doi.org/10.5004/dwt.2019.23808
69. Pathak A, Chauhan A, Stothard P, Green S, Maienschein-Cline M, Jaswal R, *et al*. Genome-centric evaluation of *Burkholderia* sp. strain SRS-W-2-2016 resistant to high concentrations of uranium and nickel isolated from the Savannah River Site (SRS), USA. Genom Data. 2017;12:62-8. https://doi.org/10.1016/j.gdata.2017.02.011
70. Zhang Y, Rodionov DA, Gelfand MS, Gladyshev VN. Comparative genomic analyses of nickel, cobalt and vitamin B12 utilization. BMC Genomics. 2009;10(1):78. https://doi.org/10.1186/1471-2164-10-78
71. Hebbeln P, Eitinger T. Heterologous production and characterization of bacterial nickel/cobalt permeases. FEMS Microbiol Lett. 2004;230(1):129-35. https://doi.org/10.1016/S0378-1097(03)00885-1
72. Pishchik V, Mirskaya G, Chizhevskaya E, Chebotar V, Chakrabarty D. Nickel stress-tolerance in plant-bacterial associations. PeerJ. 2021;9:e12230. https://doi.org/10.7717/peerj.12230
73. Xavier JC, Costa PE, Hissa DC, Melo VM, Falcão RM, Balbino VQ, *et al*. Evaluation of the microbial diversity and heavy metal resistance genes of a microbial community on contaminated environment. Appl Geochem. 2019;105:1-6. https://doi.org/10.1016/j.apgeochem.2019.04.012
74. Janssen PJ, Van Houdt R, Moors H, Monsieurs P, Morin N, Michaux A, *et al*. The complete genome sequence of *Cupriavidus metallidurans* strain CH34, a master survivalist in harsh and anthropogenic environments. PLoS One. 2010;5(5):e10433. https://doi.org/10.1371/journal.pone.0010433
75. Brito B, Prieto RI, Cabrera E, Mandrand-Berthelot MA, Imperial J, Ruiz-Argüeso T, *et al*. *Rhizobium leguminosarum hupE* encodes a nickel transporter required for hydrogenase activity. J Bacteriol. 2010;192(4):925-35. https://doi.org/10.1128/jb.01045-09
76. Huertas MJ, López-Maury L, Giner-Lamia J, Sánchez-Riego AM, Florencio FJ. Metals in cyanobacteria: Analysis of the copper, nickel, cobalt and arsenic homeostasis mechanisms. Life. 2014;4(4):865-86. https://doi.org/10.3390/life4040865
77. Schürmann J, Fischer MA, Herzberg M, Reemtsma T, Strommenger B, Werner G, *et al*. The genes *mgtE* and *spoVG* are involved in zinc tolerance of *Staphylococcus aureus*. Appl Environ Microbiol. 2024;90(6):e00453-24. https://doi.org/10.1128/aem.00453-24
78. Chen YS, Kozlov G, Fakih R, Yang M, Zhang Z, Kovrigin EL,

et al. Mg^{2+}-ATP sensing in CNNM, a putative magnesium transporter. Structure. 2020;28(3):324-35. https://doi.org/10.1016/j.str.2019.11.016

79. Franken GA, Huynen MA, Martínez-Cruz LA, Bindels RJ, de Baaij JH. Structural and functional comparison of magnesium transporters throughout evolution. Cell Mol Life Sci. 2022;79(8):418. https://doi.org/10.1007/s00018-022-04442-8
80. Hovorukha V, Moliszewska E, Havryliuk O, Bida I, Tashyrev O. Metal resistance of microorganisms as a crucial factor for their homeostasis and sustainable environment. Sustainability. 2024;16(22):9655. https://doi.org/10.3390/su16229655
81. Jin F, Sun M, Fujii T, Yamada Y, Wang J, Maturana AD, *et al*. The structure of MgtE in the absence of magnesium provides new insights into channel gating. PLoS Biol. 2021;19(4):e3001231. https://doi.org/10.1371/journal.pbio.3001231

How to cite this article:
Sivakumar K, Ramasamy SP. Role of *Enterobacter cloacae* SK1 in nickel removal and detection of nickel-resistance genes using Rapid Annotation using the Subsystem Technology server. J Appl Biol Biotech 2026;14(3):153-164. DOI: 10.7324/JABB.2026.301460